# In-situ formation of coesite in hydrothermal conditions

M. C. Wilding, C. J. Ridley, C. L. Bull, J. B. Parise

**Published version information**

**Citation:** MC Wilding et al. 'In situ formation of coesite under hydrothermal conditions.' International Journal of High Pressure Research, vol. 40, no. 4 (2020): 478-487.

**DOI:** 10.1080/08957959.2020.1830080

# *In-situ Formation of Coesite in Hydrothermal Conditions*

M. C. Wilding[a*], C. J. Ridley[b], C. L. Bull[b], J. B. Parise[c]

[a]*Department of Chemistry, University College London, 20 Gordon Street, London, WC1H 0AJ, U.K.* [b]*ISIS Neutron and Muon Facility, STFC, Rutherford Appleton Laboratory, Chilton, OXON, OX11 0QX, U.K.* [b]*Dept. of Geosciences, Stony Brook University, U.S.A.*

**ARTICLE HISTORY**
Compiled September 2, 2020

**ABSTRACT**
We present the *in situ* neutron diffraction data of a water and silica mixture at high pressure and temperature. We show initially the formation of ice VI at 1.5 GPa at 290 K in the presence of crystalline $SiO_2$, upon heating we observe its melting at ∼400 K. Upon further warming to 1200 K we observe melting of the crystalline silica. Upon cooling to 290 K and recovery to ambient pressure we obtain a mixture of silica in the coesite structure and liquid water. These results have implications for the phase diagram of the coesite–water solidus and hence the behaviour of fluids at mantle conditions.

**KEYWORDS**
High-pressure, melting, neutron diffraction, mantle, fluid

## 1. Introduction

At relatively modest pressures (1–2 GPa) the solubility of $SiO_2$ and other silicate minerals in $H_2O$ increases dramatically. Many geological processes are dominated by the interaction of minerals and volatile components such as $H_2O$ under hydrothermal conditions. For example, in the process of subduction, water and other volatile components may be released and can cause melting in the overlying mantle. The resulting high-density water-rich silica-melts, and silica-rich fluids are important in chemical transport within the earth [1, 2, 3, 4, 5, 6], and continue to be the subject of considerable research [1, 7, 8, 9]. While many of these studies have focussed on phase relations and the chemical composition of coexisting phases [10, 11, 12, 13], there have also been *in-situ* Raman studies on the silica speciation in these important geochemical fluids [14, 15, 16, 17].

The solubility of crystalline and amorphous silica (and other solutes) increases at higher pressure, such that water rich fluids become more silica rich [18, 19]. Similarly, the presence of water lowers the melting temperature of silica ($SiO_2$) and other silicate

*Corresponding author. Email: m.wilding@ucl.ac.uk

minerals, as the reactions between between silica and water become energetically more favourable [20]. At high pressures and temperatures, hydrous silicate liquids and silica-rich fluids become completely miscible as illustrated in the simplest geologically-relevant system $SiO_2$-$H_2O$.[7] The fluid ($H_2O$) saturated melting curve for silica was studied by Kennedy *et al* [7, 8, 21], this *wet solidus* was found to terminate in an invariant point, often referred to as the "second critical point", which marks the point at which the hydrous melt and aqueous fluid become indistinguishable from eachother. The trace of the apex of a melt/fluid solvus in P-T space defines a curve that separates fluid from saturated melt in the sub-critical regime, whereas only a single fluid phase is present under supercritical conditions. Figure 1 shows the dry-silica phase-diagram and the phase relations for the $SiO_2$-$H_2O$ mixed system. The *wet solidus* curve is based on the studies of Kennedy *et al.* [7] and Manning [20] which identify the regime where a homogenous fluid is present. The invariant point (second critical point) for this system is identified at 1353 K and 1 GPa. The activity-composition relations (equilibrium coefficient of reaction) have also been used to infer structural interpretations for the homogeneous fluids [20]. There is near-constant activity ($a_{SiO_2}$) of $SiO_2$ between 20 and 60 mole % $SiO_2$. At higher silica concentrations there is a change in solubility mechanics, and the activity is directly proportional to concentration. There have been a large number of studies of this and related geological relevant systems although there are few *in-situ* diffraction studies of these systems. Fluids such as these are expected to comprise of a mixture of monomers and dimers with the remaining fraction forming hydroxylated oligomers.[16, 17, 22, 23]

In the present study, neutron diffraction is used to explore the structure of $SiO_2-H_2O$ mixtures at the pressures and temperatures of the supercritical regime. The corrosive nature of water, and the requirement for relatively large sample volumes (compared to diamond anvil cell based methods) makes the study of water-rich fluids under high-PT conditions, technically very challenging. However, neutron diffraction provides a number of distinct advantages to this work, primarily the relative scattering lengths between the constituent components providing a good contrast in the data. We take advantage of recent developments in high-pressure methodology to perform an *in-situ* neutron diffraction study at elevated pressures and temperatures.

## 2. Experimental

High pressure time-of-flight (TOF) neutron powder-diffraction measurements were conducted on the PEARL high pressure instrument (ISIS Neutron and Muon Facility, UK) [24]. Crystalline $SiO_2$ ($\sim$ 10.41 mg) and liquid water ($D_2O$, $\sim$14.25 mg) were sealed in a Pt capsule (a 4 mm tall cylinder with a 2.8 mm ID, and wall thickness of 0.1 mm) using a 'tungsten in inert-gas' (TIG) welding technique. The capsule was then housed in an MgO sleeve, and loaded into a pyrophylite gasket with graphite heater assembly [25]. 50 $\mu$m thick Hf foils were placed between the MgO caps, and the Pt capsule for temperature determination. The Paris-Edinburgh press [26] with tungsten carbide (WC) anvils was used to pressurise the assembly. The sample pressure was determined from the known equation-of-state (EoS) of MgO and the temperature was determined using a calibrated Doppler line broadening of the Hf resonance with temperature [25]. The TOF diffraction data were normalised and corrected using the Mantid package [27]. An in-house correction for the wavelength and scattering-angle dependence of the neutron attenuation by the WC anvils was applied to the observed pattern. GSAS and EXPGUI were used for Rietveld refinement [28]. The scattering from the MgO, Pt capsule and

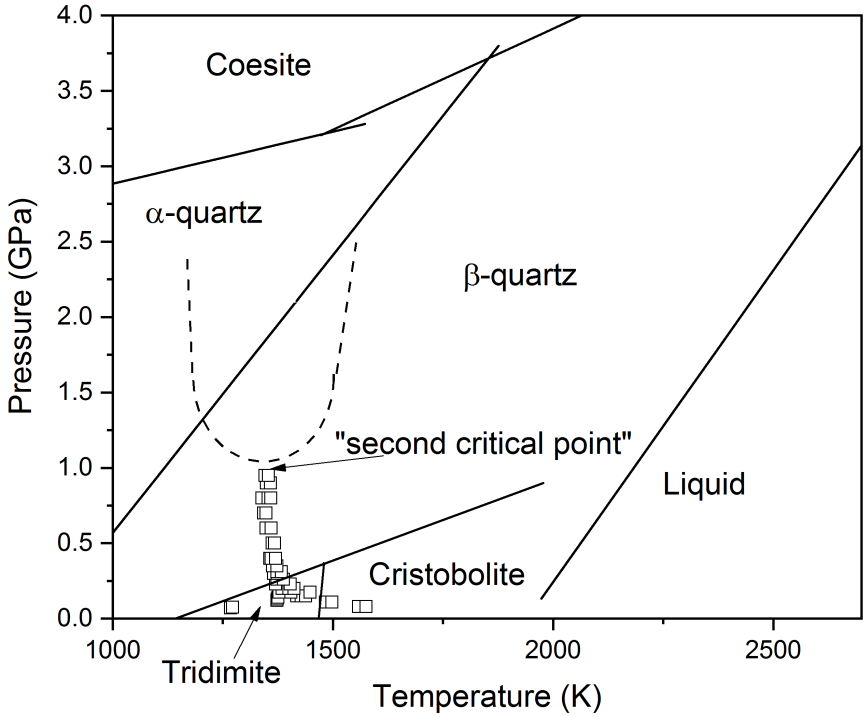


**Figure 1.** The pressure-temperature phase diagram of the binary system $SiO_2$-$H_2O$. The fluid saturated melting curve identified by Kennedy *et al* is shown as squares. [7] The critical temperature and pressure is identified at 1 GPa, 1353 K [20] above which a single homogeneous fluid exists. The dry melting curve of $\beta$ quartz is shown, based on the study of Hudon et al (2002) [30] and the $\alpha$ to $\beta$ quartz transition and quartz-coestite transitions are based on Mirwald and Massone [31]. Also shown are the positions of the quartz coesite transition from Bose *et al* [32] and from Bohlen and Boettcher [33].

the anvil materials (WC and Ni binder) were accounted for by additional crystalline phases in the Rietveld refinements.

Additional neutron powder-diffraction patterns were obtained from the recovered sample out-with the Pt capsule, using the Polaris instrument (ISIS Neutron and Muon Source, UK) [29]. The Time-of-flight diffraction pattern was collected from the sample held in a 1 mm diameter quartz glass capillary in vacuum. Data acquisition time was of the order of 12 hours.

Raman spectra were measured for all samples at ambient temperature. Spectra were recorded in backscattering using an in-house system comprising a Princeton Instruments SP2500i spectrometer equipped with a 1800 g holographic blaze grating. A diode laser ($\lambda = 532$ nm) was focused using a 20x Mitutoyu objective lens with a laser power of 5 mW at the sample position.

## 3. Results

### *3.1. In-situ Neutron Diffraction*

Figure 2b shows the *in situ* neutron diffraction pattern of the as loaded mixture of $SiO_2$ and $D_2O$ at room temperature at a pressure of 1.5 GPa. At these conditions $D_2O$ solidifies into crystalline ice VI with a tetragonal structure [34]. Rietveld analysis of the patterns gives the ratio of $SiO_2$ to $D_2O$ as 24% $SiO_2$ (by mass of capsule prior to loading was estimated to be 37% the difference in these two values is likely due to the illuminated sample volume visible by the detectors being less than the total sample volume in the capsule.). Upon heating to ∼400 K the ice melted (as shown by the disappearance of the crystalline ice reflections) and a liquid signal in the diffraction pattern appears (Figure 2c) leaving only crystalline $\alpha$-$SiO_2$ [35] and and diffraction peaks from the Pt capsule and WC anvils. Upon further heating to 1200 K (close to the limit possible with the graphite heater assembly) no melting or changes in the crystalline $SiO_2$ is observed, however, upon compression at this temperature the crystalline $SiO_2$ reflections are also lost, leaving a more intense and modified liquid signal (Figure 2d). Thus at 1200 K and 3.5 GPa we measure a liquid mixture of $SiO_2$ and $D_2O$. The liquid was quenched at high pressure by gradually reducing the applied power to the furnace. The sample pressure was then reduced back to ambient pressure. Upon recovery to ambient temperature and pressure, some crystalline reflections reappear but are different to those observed prior to heating. This result is in contrast to the recent work of Urakawa *et al* who rapidly quenched (1000 K $s^{-1}$) a mixture of $D_2O$ and quartz $SIO_2$ from a pressure of 3 GPa and 1873 K and formed hydrous $SiO_2$ glass.[36]

As a result of the high attenuation of the WC anvils, small sample volume, inherently weak scattering from non-crystalline samples and the difficulty in measuring a suitable background [1], full correction of the liquid signal is not possible, and to obtain a reproducible diffraction pattern of the pure liquid-signal *in situ* at high pressure and temperature could not be obtained.

### *3.2. Recovery of Sample*

Following the high pressure, high temperature experiment the gasket assembly was retrieved, and the Pt capsule recovered and removed the surrounding MgO (as far as possible). This was then placed into a V canister and the diffraction pattern obtained on the PEARL instrument (Figure 3a). The pattern is dominated by the scattering from the Pt capsule. However, small reflections are observed beyond ∼2.3 Å which are not those of crystalline quartz $SiO_2$. These instead index on a monoclinic crystal structure similar to that of coesite (refined lattice parameters of a=7.151(7) Å, b=12.350(9) Å, c=7.175(4) Å and $\beta$=120.28(5)° in the $C2/c$ monoclinic space group and similar to that reported previously[37]), see Figure 3. There is also a small non-crystalline profile to the background of the diffraction pattern indicating either a glassy or liquid sample is present. The Pt capsule was then opened in controlled conditions, and liquid water was observed escaping the capsule, see Figure 3b. The capsule was then opened further and clear crystallites were found within (Figure 3b). The Raman spectrum of the solid phase was then obtained and is shown in Figure 3c. The Raman spectrum is in good agreement with that reported previously for naturally occurring coesite, and is distinctly different

[1] Reconstruction of a suitable high temperature gasket assembly with similar scattering contribution of materials proved difficult to achieve satisfactorily, due to the highly plastic deformation of the pyrophyllite, and deformation of the furnace components.

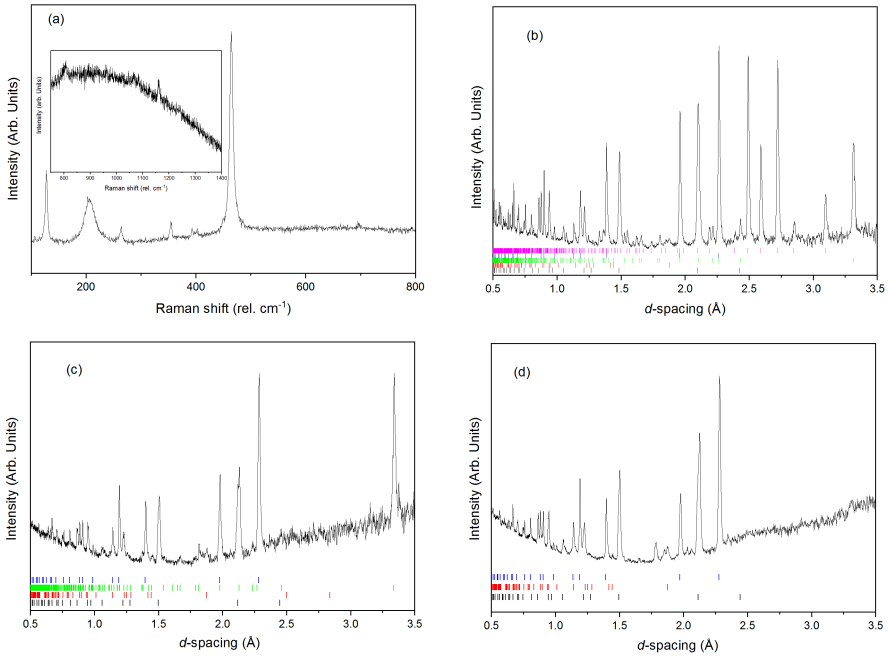


**Figure 2.** *In situ* characterisation of silica and water interaction. (a) Raman of powdered crystalline quartz structured $SiO_2$. (b) Neutron diffraction pattern of crystalline quartz $SiO_2$ and ice VI ($D_2O$) within the PE press at 1.5 GPa and 290 K. (c) Neutron powder diffraction pattern of crystalline $SiO_2$ and liquid $D_2O$ at 1.5 GPa and 400 K. (d) Neutron diffraction pattern of liquid $SiO_2$ and $D_2O$ at 3.5 GPa and 1200 K. In panels b-d the vertical tick marks show the reflection positions from (bottom to top) MgO (black), WC (red), $SiO_2$(green), Pt (blue) and $D_2O$ ice VI (magenta).

to that of the starting crystalline quartz $SiO_2$ (Figure 2a).

The recovered sample was then ground into a powder, placed in a glass quartz capillary, and the diffraction pattern measured on the POLARIS instrument at ambient conditions, see Figure 3d.[29] The glass capillary itself provides a structured background, which is quite dominant in the pattern due to the small recovered sample volume ($\sim$10 $mm^3$). It is, however, clear that the sample consists of only crystalline monoclinic coesite as shown by the tick mark indexing of the pattern in Figure 3d. The coesite structure, as previously determined by Smyth *et al* [37], was Rietveld refined against the diffraction pattern (Figure 3d), and the refined structural values are reported in Table 1. Considering the above limitations, these values are in good agreement with those reported from single crystal X-ray diffraction (Smyth *et al*) of naturally occurring coesite, which are also reported in Table 1).

## 4. Discussion

Within the level of detection we are unable to see any demonstrable crystalline reflections in the *in situ* diffraction pattern of $D_2O$ and $SiO_2$ at 3.5 GPa and 1200 K. This would imply that there is only liquid present in the illuminated sample volume. We note that the neutron scattering of the liquid will be weak, compounded in the presence of the strongly scattering anvils and background inherent to the gasket material. However, even with the high counting statistics (in excess 24 hours for this data point) no crystalline reflections from $SiO_2$ are observed. The most intense reflections from coesite at 3.5 GPa are the $20\bar{2}$, 002, 040 reflections (each with similar intensity) all centred at $\sim$ 2.93 Å (based upon the non-uniform axial compression of the crystalline structure [38]). However, we see no evidence of such reflections in the *in situ* diffraction pattern. This observation of liquid $SiO_2$ and $D_2O$ at 3.5 GPa and 1200 K has implications for the phase boundary of coesite formation in the presence of water as it starts to show that the $SiO_2$ melting curve is depressed by the presence of water (as expected) and to our knowledge is the first *in situ* experimental data point adding to the phase diagram in this region. As we first cooled the sample slowly the $SiO_2$ crystallised out of the melt into the stable phase at this pressure resulting in coesite in the presence of water. This would suggest the presence of a second critical point for coesite, and a region of complete miscibility between a silicate liquid and an aqueous fluid. There is however, no available experimental data to indicate how the supercritical region for the two crystalline $SiO_2$ phases are related.

Coesite, the high-pressure polymorph of $SiO_2$, is a framework silicate that comprises of four-membered rings aligned in chains parallel to the c-axis; interactions between these chains result in the formation of 6- and 8-membered rings. Shorter distances between the oxygen atoms of the linked $SiO_4$ tetrahedra mean that the structure is denser than either quartz or cristobalite [37]. There are two non-equivalent $SiO_4$ tetrahedra and eight Si-O distances [39] and cristobalite can be viewed as a disordered phase closely resembling an amorphous structure of linked tetrahedral units. Indeed, it has been reported that cristobalite can nucleate and grow metastably from hydrous gels at ambient pressure [40]. More recently it has been shown how the amorphous forms of $SiO_2$ are related structurally to the crystalline forms in terms of connectivity and networks, by comparison of diffraction patterns.[41] Coesite can be synthesised hydrothermally [42] at the temperatures and pressures accessed by this experiment and the depression of the melting point of coesite in the presence of water is consistent with the explorations of phase relations of $SiO_2$ and $NaAlO_2$ in the presence of water [31, 43]; the addition of

**Table 1.** Determined crystallographic parameters determined form synthetic coesite (this study) compared to that determined previously by Smyth *et al* from naturally occurring coesite [37].

| Parameter | Synthetic | | | Natural | | |
|---|---|---|---|---|---|---|
| $a$ (Å) | 7.1379(17) | | | 7.1464(9) | | |
| $b$ (Å) | 12.375(2) | | | 12.3796(19) | | |
| $c$ (Å) | 7.1738(14) | | | 7.1829(8) | | |
| $\beta$ (°) | 120.336(15) | | | 120.351(12) | | |
| $V$ (Å$^3$) | 546.92(11) | | | 548.76(22) | | |
| Atom | $x$ | $y$ | $z$ | $x$ | $y$ | $z$ |
| Si1 | 0.149(4) | 0.100(3) | 0.064(5) | 0.14302(4) | 0.10832(2) | 0.07231(4) |
| Si2 | 0.504(6) | 0.161(3) | 0.534(5) | 0.50677(4) | 0.15800(2) | 0.54073(4) |
| O1 | 0 | 0 | 0 | 0 | 0 | 0 |
| O2 | 0.5 | 0.119(2) | 0.75 | 0.5 | 0.11643(7) | 0.75 |
| O3 | 0.272(4) | 0.117(2) | 0.946(4) | 0.26400(11) | 0.12452(6) | 0.93830(11) |
| O4 | 0.306(3) | 0.0978(17) | 0.323(3) | 0.31144(12) | 0.10379(6) | 0.32785(12) |
| O5 | 0.017(3) | 0.2153(15) | 0.489(3) | 0.01746(11) | 0.21192(5) | 0.47851(12) |

water to the Na-Al-Si-O system results in complete melting at 3 GPa, 1300 K. It is easy to envisage how coesite would nucleate from a high-density fluid; the silica-rich fluids comprise $H_4SiO_4$ monomers which become progressively polymerised as the $SiO_2$ content increases[16, 17, 9, 20]. Evidence supporting this concept includes the near constant activity of $SiO_2$ close to the critical region [9], and the formation of stable $Si_nO_n(OH)_{2n}$ ring structures, hydrogen-bonded to adjacent rings. There is further evidence from simulation and experiment to indicate the formation of stable $Si_nO_n(OH)_{2n}$ rings [22, 23]. It is clear, therefore, to see energetic pathways to the formation of the crystalline phase coesite, comprising different-membered rings, from a high-density fluid with a similar but more disordered distribution of rings and polymerised hydrous silicate species.

## 5. Conclusions

We have performed neutron diffraction measurements *in situ* on a mixture of $D_2O$ and crystalline $SiO_2$ at high temperatures and pressures. The pressure and temperatures accessed (3.5 GPa and 1200 K) lies within the coesite stability field but there is no evidence for the presence of crystalline coesite *in situ*. We are confident that at the highest pressures and temperatures achieved we have accessed a liquid phase, shown by the progressive disappearance of characteristic Bragg reflections of $\alpha$-quartz and crystalline ice. We were unable to obtain the structure of the fluid phase in this current experiment; measurement and evaluation of the liquid structure in the future is the ultimate goal of these types of hydrothermal fluid experiments as progress in anvil and gasket developments are made. The conditions of 1200 K and 3.5 GPa suggest we are within the stability field of crystalline coesite however, within the limits of the diffraction signal *in situ*, no crystalline coesite is present and we are led to conclude that in these conditions the stable phase is a silica rich fluid consistent with the depression of the melting point of coesite in the presence of water, and we provide the first experimentally determined data point for the pressure temperature region of its existence. Upon slow cooling, coesite nucleates and is recovered together with excess $D_2O$.

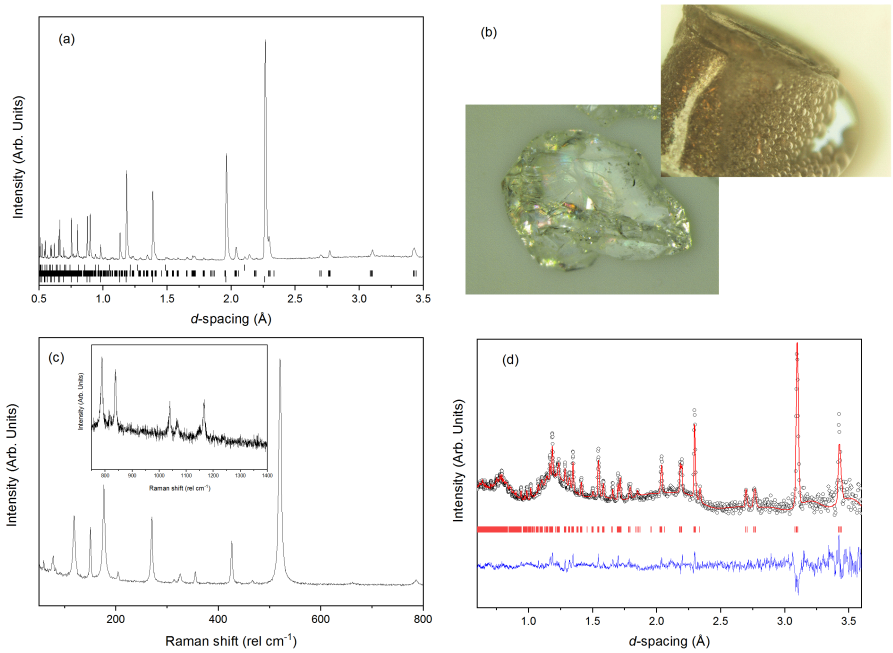


**Figure 3.** Characterisation of recovered coesite sample. (a) Neutron powder diffraction pattern of recovered sample within Pt capsule. Vertical tick marks show the indexed position of Pt, crystalline $SiO_2$ (in the coesite structure), and MgO (top to bottom). Also present is a liquid water signal in the background signal as a broad feature centered around 3 Å. (b) Top right image of just opened Pt capsule with water escaping form the opening and bottom left a piece of the recovered $SiO_2$ solid. (c) Raman spectra of solid recovered from Pt capsule. (d) Neutron diffraction pattern of recovered crystalline phase (measured within a glass capillary). The black circles are data points, red line is the Rietveld fit to the data, the blue trace the residual of the fit to the data and the red tick marks are the expected reflection positions for the coesite.

## 6. Acknowledgments

The authors thank STFC for providing access to the PEARL instrument and facilties within ISIS. We thank Ron Smith of ISIS, STFC for help in obtaining the data on POLARIS.

## References

[1] O. Elazar, D. Frost, O. Navon, and R. Kessel, *Melting of $H_2O$ and $CO_2$-bearing eclogite at 4-6 GPa and 900-1200 degrees C: Implications for the generation of diamond-forming fluids*, Geochimica et Cosmochimica Acta 255 (2019), pp. 69–87.

[2] Y. Weiss, R. Kessel, W.L. Griffin, I. Kiflawi, O. Klein-BenDavid, D.R. Bell, J.W. Harris, and O. Navon, *A new model for the evolution of diamond-forming fluids: Evidence from microinclusion-bearing diamonds from Kankan, Guinea*, LIithos 112 (2009), pp. 660–674 9th International Kimberlite Conference, Johann Wolfgang Goethe Univ, Frankfurt, Germany Aug 10-15, 2008.

[3] J. Hermann, C. Spandler, A. Hack, and A.V. Korsakov, *Aqueous fluids and hydrous melts in high-pressure and ultra-high pressure rocks: Implications for element transfer in subduction zones*, Lithos 92 (2006), pp. 399–417.

[4] B. Mysen, *Silicate solution, cation properties, and mass transfer by aqueous fluid in the Earth's interior*, Progress in Earth and Planetary Science 5 (2018).

[5] Mysen, B, *Structure-property relationships of COHN-saturated silicate melt coexisting with COHN fluid: A review of in-situ, high-temperature, high-pressure experiments*, Chemical Geology 346 (2013), pp. 113–124.

[6] C.E. Manning, *Fluids of the Lower Crust: Deep Is Different*, in *Annual Review of Earth and Planetary Sciences,* , , in *Annual Review of Earth and Planetary Sciences,* , ed. Jeanloz, R and Freeman, K HJeanloz, R and Freeman, K H ed., , 2018, pp. 67–97.

[7] G.C. Kennedy, H.C. Heard, G.J. Wasserburg, and R.C. Newton, *Upper 3-Phase Region In System $SiO_2$–$H_2O$*, American Journal of Science 260 (1962), pp. 501–521.

[8] G. Kennedy, G. Wasserburg, and H. Heard, *The Upper 3-Phase Region In The System $SiO_2$-$H_2O$*, Journal of Geophysical Research 64 (1959), p. 1111.

[9] C.E. Manning, *The Solubility Of Quartz In $H_2O$ In The Lower Crust And Upper-Mantle*, Geochimica et Cosmochimica Acta 58 (1994), pp. 4831–4839.

[10] J. Walther and P. Orville, *The Extraction Quench technique for Determination of the Thermodynamic Properties of Solute Complexes-Application to Quartz Solubility in Fluid Mixtures*, American Mineralogist 68 (1983), pp. 731–741.

[11] R.C. Newton and C.E. Manning, *Hydration state and activity of aqueous silica in $H_2O$-$CO_2$ fluids at high pressure and temperature*, American Mineralogist 94 (2009), pp. 1287–1290.

[12] M.F. Cruz and C.E. Manning, *Experimental determination of quartz solubility and melting in the system $SiO_2$-$H_2O$-NaCl at 15-20 kbar and 900-1100 degrees C: implications for silica polymerization and the formation of supercritical fluids*, Contributions to Mineralogy and Petrology 170 (2015).

[13] R. Zhang, X. Zhang, and S. Hu, *Dissolution kinetics of quartz in water at high temperatures across the critical state of water*, Journal of Supercritical Fluids 100 (2015), pp. 58–69.

[14] B.O. Mysen, K. Mibe, I.M. Chou, and W.A. Bassett, *Structure and equilibria among*

*silicate species in aqueous fluids in the upper mantle: Experimental $SiO_2$-$H_2O$ and MgO-$SiO_2$-$H_2O$ data recorded in situ to 900 degrees C and 5.4GPa*, Journal of Geophysical Research-Solid Earth 118 (2013), pp. 6076–6085.

[15] B.O. Mysen, *Silicate-COH melt and fluid structure, their physicochemical properties, and partitioning of nominally refractory oxides between melts and fluids*, Lithos 148 (2012), pp. 228–246.

[16] N. Zotov and H. Keppler, *Silica speciation in aqueous fluids at high pressures and high temperatures*, Chemical Geology 184 (2002), pp. 71–82.

[17] Zotov, N and Keppler, H, *In-situ Raman spectra of dissolved silica species in aqueous fluids to 900 degrees C and 14 kbar*, American Mineralogist 85 (2000), pp. 600–603.

[18] R.O. Fournier, *The solubility of amorphous silica in water at high temperature and high pressures*, American Mineralogist 62 (1977), pp. 1052–1056.

[19] F. Holtz, J. Roux, H. Beherens, and M. Pichavant, *Water solubility in silica and quartzfeldspathic melts*, American Mineralogist 85 (2000), pp. 682–686.

[20] R.C. Newton and C.E. Manning, *Thermodynamics of $SiO_2$-$H_2O$ fluid near the upper critical end point from quartz solubility measurements at 10 kbar*, Earth And Planetary Science Letters 274 (2008), pp. 241–249.

[21] G. Wasserburg, *The Effects of $H_2O$ in Silicate Systems*, Journal of Geology 65 (1957), pp. 15–23.

[22] G. Spiekermann, M. Wilke, and S. Jahn, *Structural and dynamical properties of supercritical $H_2O$-$SiO_2$ fluids studied by ab initio molecular dynamics*, Chemical Geology 426 (2016), pp. 85–94.

[23] G. Spiekermann, M. Steele-MacInnis, C. Schmidt, and S. Jahn, *Vibrational mode frequencies of silica species in $SiO_2$-$H_2O$ liquids and glasses from ab initio molecular dynamics*, Journal of Chemical Physics 136 (2012).

[24] C.L. Bull, N.P. Funnell, M.G. Tucker, S. Hull, D.J. Francis, and W.G. Marshall, *PEARL: the high pressure neutron powder diffractometer at ISIS*, High Pressure Res. 36 (2016), pp. 493–511.

[25] Y. Le Godec et al., *Neutron diffraction at simultaneous high temperatures and pressures, with measurement of temperature by neutron radiography*, Mineral. Mag. 65 (2001), pp. 737–748.

[26] J.M. Besson, R.J. Nelmes, G. Hamel, J.S. Loveday, G. Weill, and S. Hull, *Neutron powder diffraction above 10 GPa*, Physica B 180 (1992), pp. 907–910.

[27] O. Arnold et al., *Mantid—Data analysis and visualization package for neutron scattering and $\mu$SR experiments*, Nucl. Instrum. Meth. A 764 (2014), pp. 156–166.

[28] B.H. Toby, *EXPGUI, a graphical user interface for GSAS*, J. Appl. Crystallogr. 34 (2001), pp. 210–213.

[29] R.I. Smith, S. Hull, M.G. Tucker, H.Y. Playford, D.J. McPhail, S.P. Waller, and S.T. Norberg, *The upgraded Polaris powder diffractometer at the ISIS neutron source*, Review of Scientific Instruments 90 (2019), p. 115101.

[30] P. Hudon, I. Jung, and D.R. Baker, *Melting of beta-quartz up to 2.0 GPa and thermodynamic optimization of the silica liquidus up to 6.0 GPa*, Physics Of The Earth And Planetary Interiors 130 (2002), pp. 159–174.

[31] Mirwald, P W, *Experimental re-examination of the phase transition quartz-coesite - The reaction in presence of $H_2O$ and at anhydrous conditions*, Geochimica et Cosmochimica Acta 71 (2007), p. A672 17th Annual V M Goldschmidt Conference, Cologne, Germany Aug, 2007.

[32] K. Bose and J. Ganguly, *Quartz-Coesite transition revisited - reversed experimental-determination at 500-1200 degrees C and retrieved thermochemical properties*,

American Mineralogist 80 (1995), pp. 231–238.
[33] S. Bohlen and A. Boettcher, *The quartz–reversible–coesite transformation – a precise determination and the effects of other components*, Journal of Geophysical Research 87 (1982), pp. 7073–7078.
[34] W.F. Kuhs, J.L. Finney, C. Vettier, and D.V. Bliss, *Structure and hydrogen ordering in ices VI, VII, and VIII by neutron powder diffraction*, The Journal of Chemical Physics 81 (1984), pp. 3612–3623.
[35] G.A. Lager, J.D. Jorgensen, and F.J. Rotella, *Crystal structure and thermal expansion of $\alpha$-quartz $SiO_2$ at low temperatures*, Journal of Applied Physics 53 (1982), pp. 6751–6756.
[36] S. Urakawa, T. Inoue, T. Hattori, A. Sano-Furukawa, S. Kohara, D. Wakabayashi, T. Sato, N. Funamori, and K.i. Funakoshi, *X-ray and Neutron Study on the Structure of Hydrous SiO2 Glass up to 10 GPa*, Minerals 10 (2020).
[37] J.R. Smyth, J.V. Smith, G. Artioli, and A. Kvick, *Crystal structure of coesite, a high-pressure form of silica, at 15 and 298 K from single-crystal neutron and x-ray diffraction data: test of bonding models*, The Journal of Physical Chemistry 91 (1987), pp. 988–992.
[38] R. Angel, J. Mosenfelder, and C. Shaw, *Anomalous compression and equation of state of coesite*, Physics of the Earth and Planetary Interiors 124 (2001), pp. 71 – 79.
[39] G.V. Gibbs, C.T. Prewitt, and K.J. Baldwin, *Study of structural chemistry of coesite*, Zeitschrift fur Kristallographie 145 (1977), pp. 108–123.
[40] J.R. Martinez, A. Vasquez-Duran, G. Martinez-Castanon, G. Ortega-Zarzosa, S.A. Palomares-Sanchez, and F. Ruiz, *Coesite formation at ambient pressure and low temperatures*, Advances in Materials Science and Engineering (2008).
[41] Y. Onodera et al., *Understanding diffraction patterns of glassy, liquid and amorphous materials via persistent homology analyses*, Journal of the Ceramic Society of Japan 127 (2019), pp. 853–863.
[42] J. Arndt and N. Rombach, *Synthesis of Coesite from Aqueous Solutions*, Journal of Crystal Growth 35 (1976), pp. 28–32.
[43] P. Mirwald and H. Massonne, *The low-high quartz and quartz-coesite transition to 40 kbar between 600-degrees-C and 1600-degrees-C and some reconnaissance data on the effect of $NaAlO_2$ component on the low quartz-coesite transition*, Journal of Geophysical Research 85 (1980), pp. 6983–6990.